NANOCRYSTALLINE GOLD CERIA-BASED WATER –GAS SHIFT CATALYSTS FOR FUEL CELL APPILICATIONS

Ivan C. Lee and Deryn Chu

AMSRD-ARL-SE-DC
US Army Research Laboratory
2800 Powder Mill Road
Adelphi, MD 20904

Abstract

New gold/ceria-based water-gas shift (WGS) catalysts have been developed to clean up carbon monoxide in hydrogen-rich gas for fuel cell applications. The new water-gas shift catalyst, $Au/MgO/Ce_{0.8}Sm_{0.15}Gd_{0.05}O_{1.9}$, is non-pyrophoric and has high WGS activities at low temperature (below 300 ^oC) with $H_2/CO=1$ in the feed. This nanocystalline(<10nm) $Au/MgO/Ce_{0.8}Sm_{0.15}Gd_{0.05}O_{1.9}$ catalyst was synthesized by carbonate co-precipitation of doped ceria followed by gold deposition with urea. The durability of Sm- and Gd-doped ceria as low-temperature water-gas shift (WGS) catalysts was tested with argon gas saturated with water at elevated catalyst temperatures. The SEM and BET surface area analysis indicated that there were no significant changes at 350°C for 10 hours. We have evaluated the WGS activities of various ceria-based catalysts containing Au, Sm, Gd, Zr and Mg at CO/H2= 1. Our results indicate that the presence of Au and MgO in $Au/MgO/Ce_{0.8}Sm_{0.15}Gd_{0.05}O_{1.9}$ plays significant roles in the WGS reaction. No methane is produced in our studies.

Introduction

An integrated system of a fuel reformer and a fuel cell can provide portable and mobile power for battery chargers and scout vehicle silent watch. Diesel fuel reformers produce hydrogen for fuel cells[1,2]. Unfortunately, the diesel fuel reformers also produce appreciable amount of CO. For instance, catalytic partial oxidation gives ~ 48 % CO (N_2-free and dry basis)[1], while steam reforming produces 16% CO (dry basis)[2]. Since the tolerable level of carbon monoxide in PEM fuel cells is about 10 ppm, one or several intermediate carbon monoxide cleanup steps (such as water-gas shift reactor) are necessary.

The primary objective is to develop a novel low temperature water-gas shift catalyst to clean up carbon monoxide in the hydrogen-rich reformate. The water-gas shift (WGS) reaction ($CO + H_2O \rightleftharpoons CO_2 + H_2$) currently attracts lots of attention because the deactivation of commercial $Cu/ZnO/Al_2O_3$ water-gas shift catalysts is a major technical barrier for fuel processors. Gold/ceria-based catalysts can potentially replace the copper-based catalysts for water-gas shift reaction[3-7]. However, there have been some controversies on the reducibility of ceria[8] and the deactivation of gold/ceria materials[9].

This paper summarizes our recent research efforts to develop metal/doped-ceria as low-temperature WGS catalysts. Our approach for water gas shift catalyst development is to prepare nanocrystalline ceria-based catalysts, and then measure the catalyst activity with realistic reformate compositions (H_2/CO ratio =1). Oxides of Mg, Zr, as well as lanthanides, such as Ce, Sm and Gd, have been chosen as support materials in this study.

Experimental

Material Synthesis. The synthesis of gold catalyst was a two-step process. First, nanocrystalline supports made of ceria doped with samarium and gadolinium were prepared by carbonate co-precipitation. Next, gold nanocrystallites were deposited onto doped ceria support materials by deposition-precipitation with urea.

Doped ceria support materials were produced via co-precipitation using ammonium carbonate and solutions of 0.15 M $Ce(NO_3)_3$, $Sm(NO_3)_3$ and $Gd(NO_3)_3$. Typically, 80 cm^3 of $Ce(NO_3)_3$, 15 cm^3 of $Sm(NO_3)_3$ and 5 cm^3 of $Gd(NO_3)_3$ were added into 100 cm^3 of 1.5 M ammonium carbonate solution. The mixture was stirred continuously and was controlled at 65°C by a circulated water bath. The resultant suspension was homogenized and then filtered under vacuum. The precipitate was washed with de-ionized water and then with ethanol. The precipitate was allowed to dry overnight. Finally, it was crushed and was calcined in a tube furnace under flowing O_2 (150 cc/min) at 600°C. The ramping and cooling rates of the furnace were controlled at 5°C/min. The calcination temperature of 600°C was chosen based on our thermogravimetric analysis (TGA) with a Perkin Elmer TGA7 analyzer.

Characterization. X-ray diffraction (XRD) measurements were performed using a Philips PW 1840 diffractometer operated at 40 kV/20 mA. Line broadening analysis of <220> and <111> planes determined the crystallite sizes of doped ceria and gold, respectively.

Multi-point BET surface areas of the water-gas shift materials were determined with a Micromeritics ASAP 2010 Automatic Physisorption Analyzer. The samples were degassed at 250°C, and the sample tubes were backfilled with nitrogen. Then 11 equilibrium data points of nitrogen adsorption were taken at relative pressures between 0.05 and 0.3.

The material morphology and elemental composition analysis were performed with a Hitachi S4500 field-emission scanning electron microscope (SEM) equipped with an energy dispersive X-ray spectrometer (EDX). The sample morphology was further examined with a JEOL 2010 transmission electron microscope (TEM) operated at 200 kV. High resolution images show lattice fringes and allow the examination of particle size and crystalline structure. The sample powder was suspended in ethanol using a ultrasonic bath and was deposited on a 400-mesh Cu grid.

Durability and Activity Tests. The durability of the gold catalyst was tested by flowing humidified argon at an elevated temperature. 75.0 sccm of argon was saturated with H_2O with a gas bubbler at 76.2^{o}C. This corresponds to about 50 sccm of water vapor. This humidified argon stream was fed into a quartz tube with 0.2 g of supported gold catalyst in a tube furnace at 350°C for 3 or 10 hours. Then the catalysts were analyzed with SEM, TEM and BET surface area measurements.

We measured the reaction rates for WGS at atmospheric pressure with powder catalysts loaded at the center of a ¼"tubular quartz reactor. All catalysts were non-pyrophoric, and they were used as prepared without activation. We injected the water into the flowing gas stream by a HPLC liquid pump and vaporized in the heated gas line before entering the reactor. The water in the reactor exit stream was collected by an ice-water condenser. The product gas stream was then analyzed on line simultaneously by two columns of an Agilent 3000 micro-gas chromatograph. A molecular sieve column (using argon as carrier gas) separates the carbon monoxide, hydrogen and methane; the Plot U column (using helium as carrier gas) separates the carbon dioxide. Then the reaction rate was calculated by the carbon dioxide product, and the rate was normalized by the weight of catalyst.

Results and Discussion

Tables 1 and 2 illustrate some characterization results of the water-gas shift materials developed in this work. Our results indicate that we can produce ceria particles of less than 10 nm by carbonate (co)precipitation (Table 1). For comparison, we also synthesized ceria by thermal deposition of solid cerium nitrate hexahydrate [$Ce(NO_3)_3*6H_2O$]. We used TGA to determine the optimum calcination temperatures of all ceria materials from their precursors. The optimum calcinations temperatures were chosen based on our TGA profiles and the subsequent XRD diffraction patterns so that ceria was produced in a fluorite crystal structure.

Table 1. Characterization of Pure Ceria, $\phi = 6/(S\rho)$; Density of Pure Ceria, $\rho = 7.184$ g/cm^3

Method	Surface Area (S), m^2/g	Spherical Diameter (ϕ), nm
Thermal Decomposition	57	14.8
Carbonate (Co)Precipitation	129	6.47
Flame Synthesis	154 [10]	5.44

The XRD and BET analysis (Table 2) show that thermal decomposition (Sample II) produces ceria with larger crystallites and a smaller surface area than carbonate precipitation (Sample I). Table 2 also indicates that doping ceria with 20% of other lanthanides, such as Sm and Gd (Samples III-V), would increase the crystallite size and would decrease the surface area. The reaction temperatures of Samples IV and V are different during co-precipitation. Higher reaction temperature in Sample V increased the surface area of the doped ceria. Supported gold catalysts (Sample VI) were prepared using Sample V as the support materials.

Table 2. Characterization of Water-Gas Shift Materials.

	Materials	Crystallite Size (XRD), nm	Multipoint BET Surface Area, m^2/g
I	Ceria (Carbonate Precipitation)	4.93 <220>	129.0
II	Ceria (Thermal Decomposition)	11.8 <220>	56.6
III	$Ce_{0.8}Sm_{0.2}O_{1.9}$	5.85 <220>	85.0
IV	$Ce_{0.8}Sm_{0.15}Gd_{0.05}O_{1.9}$	9.76 <220>	79.5
V	$Ce_{0.8}Sm_{0.15}Gd_{0.05}O_{1.9}$	8.99 <220>	94.3
VI	Au/ $Ce_{0.8}Sm_{0.15}Gd_{0.05}O_{1.9}$	6.74 (Au, <111>)	103.8

Table 3. Elemental Analysis of Doped Ceria Prepared by Carbonate Co-Precipitation.

	Atomic %		
Spot #	Ce	Sm	Gd
1	78.4	16.0	5.7
2	78.2	15.8	6.1
3	80.4	14.9	4.7
Average	79.0	15.6	5.5

Elemental analysis of the doped ceria by EDX (Table 3) shows that elemental compositions of Ce, Sm and Gd in the doped ceria matches the nominal compositions of the Ce^{3+}, Sm^{3+} and Gd^{3+} in the nitrate mixture. In other words, the atomic % of Sm and Gd in ceria can be achieved by mixing the nitrate solutions in a desired volumetric ratio. This is consistent with a recent paper in which a single lanthanide element is doped in the ceria[11]. Since the XRD pattern of the doped ceria prepared in this work matched the literature pattern of a fluorite structure[7], the composition of doped ceria was assigned to be $Ce_{0.8}Sm_{0.15}Gd_{0.05}O_{1.9}$. Our inductively coupled plasma mass spectroscopy (ICP-MS) results confirmed the materials composition of our doped ceria. And the atomic absorption spectroscopy (AAS) analysis quantified the gold content in the Au/$Ce_{0.8}Sm_{0.15}Gd_{0.05}O_{1.9}$ to be 7.1 wt %. If all the gold in solution are deposited onto the ceria, the gold content of our catalyst would be 7.6 wt %.

Some of the major limitations of commercial $Cu/ZnO/Al_2O_3$ water-gas shift catalysts include the thermal aging (or sintering) and the stability with water[12,13]. A recent study has suggested some deactivation mechanism of Au/CeO_2 catalysts[9]. Here, we investigated the effects of both thermal aging and water vapor on the Au/$Ce_{0.8}Sm_{0.15}Gd_{0.05}O_{1.9}$. These effects were examined simultaneously by flowing Ar gas (saturated with water) over the Au/$Ce_{0.8}Sm_{0.15}Gd_{0.05}O_{1.9}$ that was controlled at 350°C. Table 4 summarizes the durability test results of Au/$Ce_{0.8}Sm_{0.15}Gd_{0.05}O_{1.9}$ (Sample VII). Sample VII was prepared using Sample IV as the support material. The BET analysis showed that flowing humidified Ar over the Au/$Ce_{0.8}Sm_{0.15}Gd_{0.05}O_{1.9}$ at 350°C had insignificant effects on the BET surface area (Table 4). The change in surface area was less than 5% for 10 hours. Figure 1 illustrates a SEM image of the Sample IX. Other images of Samples IV, VII, VIII and IX with different magnifications (500x, 5000x and 50000x) are not shown here. The SEM images illustrates that there is no significant morphology difference among the samples. Particle size analysis with transmission electron microscopy (TEM) is shown in Figure 2. The TEM image suggests that the Au/$Ce_{0.8}Sm_{0.15}Gd_{0.05}O_{1.9}$ remains nanoscale after 10 hours.

Table 4. Durability of Au/ $Ce_{0.8}Sm_{0.15}Gd_{0.05}O_{1.9}$ under Humidified Argon Treatment at 350°C.

	Materials	Duration for Humidified Ar Treatment (hrs.)	Multipoint BET Surface Area, m^2/g
IV	$Ce_{0.8}Sm_{0.15}Gd_{0.05}O_{1.9}$	0	79.5
VII	Au/$Ce_{0.8}Sm_{0.15}Gd_{0.05}O_{1.9}$	0	75.1
VIII		3	78.7
IX		10	77.8

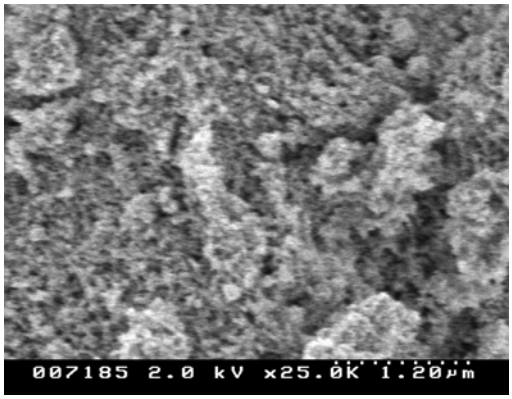

Figure 1. SEM micrograph of Au/ $Ce_{0.8}Sm_{0.15}Gd_{0.05}O_{1.9}$ treated with humidified Ar for 10 hrs at 350 ^oC (Sample IX).

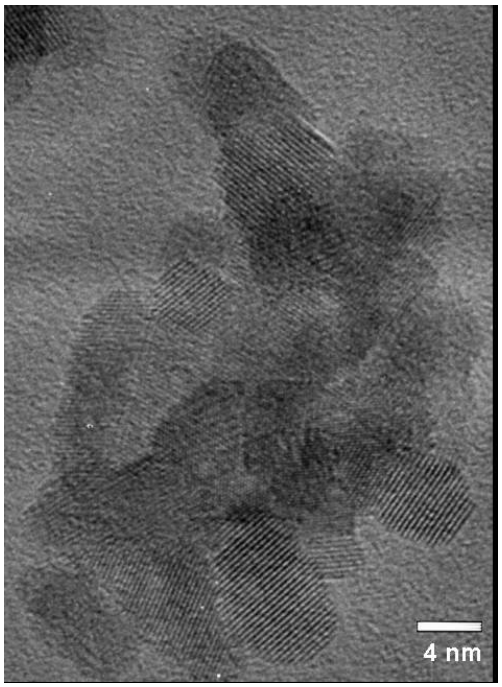

Figure 2. TEM micrograph of Au/ $Ce_{0.8}Sm_{0.15}Gd_{0.05}O_{1.9}$ treated with humidified Ar for 10 hrs at 350 ^oC (Sample IX).

The WGS reaction rates of ceria-based samples are compared in Figure 3. We kept the conversion < 10% and the pressure drop < 10 psig in all cases. Therefore, the catalyst bed temperature can be assumed to be constant, and mass transfer-free operating conditions are established for each temperature. We observe no methane in all our experiments. The BET surface area analysis results are shown in Table 5.

The activities of two Au/CeO2 catalysts are shown in Figure 3. The difference is the preparation of ceria, while the conditions of gold deposition are the same. Sample XI has a larger surface area and higher activity than Sample XII (Figure 3 and Table 5).

Although surface area and crystallite size are generally believed to be two of the major factors for catalytic activities, dopants in Ce crystal structure also play critical roles in the WGS activity. This work shows that nanocystalline (< 10 nm, XRD) Au/$Ce_{0.8}Sm_{0.15}Gd_{0.05}O_{1.9}$ with high surface area (>100 m^2/g) can be synthesized by carbonate co-precipitation followed by deposition with urea. As indicated in Tables 1 and 2, the surface area and the crystallite size are process-dependent. On the other hand, Au/$Ce_{0.8}Sm_{0.15}Gd_{0.05}O_{1.9}$ has a higher surface area than Au/$Ce_{0.75}Zr_{0.25}O_2$ (Table 4), but the latter is a better WGS catalyst below 400 ^oC (Figure3). To elucidate other important parameters, we have investigated the WGS activities of Mg-, Sm-, Gd- and Zr-doped ceria (Figure 3).

We demonstrated earlier that the additions of Sm and Gd into Ce crystal structure thermally stabilize the material, but these dopants apparently hinder the oxygen mobility (below 400°C). In contrast, Zr seems to improve both thermal resistance of the ceria and oxygen storage/release capacity. This is consistent with some general understanding of Ce-Zr materials[14,15]. On the other hand, Au/MgO has been shown to be a very active catalyst for CO oxidation[16], but there is no published result on its WGS activity. Here our results indicate that doping Mg into $Ce_{0.8}Sm_{0.15}Gd_{0.05}O_{1.9}$ structure greatly improves the WGS activity of Au/ $Ce_{0.8}Sm_{0.15}Gd_{0.05}O_{1.9}$. This implies that MgO improves the oxygen transport and the CO oxidation step in the WGS reaction. The TEM image of our Au/MgO/$Ce_{0.8}Sm_{0.15}Gd_{0.05}O_{1.9}$ is shown in Figure 4. The activity of this catalyst is shown in Figure 3.

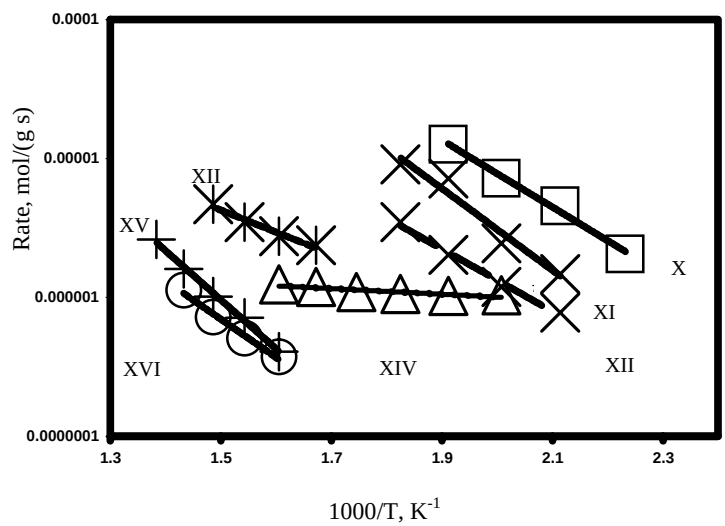

Figure 3. An Arrhenius plot for the water-gas shift rates on ceria-based catalysts (Samples X to XVI, Table 5). (Inlet gas contains 5%CO and 5%H_2, and H_2O(g)/CO=5.)

The significance of this work is that we have developed a non-pyrophoric low temperature WGS catalyst for fuel processor. Our catalysts have two important characteristics. First, all the catalysts shown in Figure 4 are not sensitive to air (i.e. non-pyrophoric) while typical Cu/ZnO/Al_2O_3 catalysts are air sensitive. In contrast to industrial plants, this feature is particularly important for objective force applications because these applications involve frequent on-off cycles during which air enters the system. Using non-pyrophoric materials often means a safer system. Another important characteristic is that our catalysts show high activities at H_2/CO ratio = 1. Previously, most of the water-gas shift catalyst research projects

focus on gas feed at very low or in absence of hydrogen. Only recently the literature[3,8] shows some interests in the water-gas shift catalyst that works at a reasonable hydrogen level (relative to CO). Note that hydrogen is the main fuel for fuel cell applications, particular polymer electrolyte membrane (PEM) fuel cells. Fuel processors break down the hydrocarbon fuel into reformate which contains smaller molecules including H_2, CO and others. Here we have tailored our catalysts at H_2/CO =1 which is realistic for catalytic partial oxidation of diesel fuel[1].

Table 5. Characterization of Ceria-Based WGS Catalysts Shown in Figure 3.

Sample	Materials	Preparation Method of Ceria or Doped Ceria	Multipoint BET Surface Area, m^2/g
X	$Au/MgO/Ce_{0.8}Sm_{0.15}Gd_{0.05}O_{1.9}$	Carbonate Coprecipitation	73.4
XI	Au/CeO_2	Carbonate Coprecipitation	94.9
XII	Au/CeO_2	Thermal Decomposition	70.1
XIII	$Au/Ce_{0.75}Zr_{0.25}O_2$	Sol gel	57.9
XIV	CeO_2	Carbonate (Co)Precipitation	129.0
XV	$Au/Ce_{0.8}Sm_{0.15}Gd_{0.05}O_{1.9}$	Carbonate Coprecipitation	103.8
XVI	$MgO/Ce_{0.8}Sm_{0.15}Gd_{0.05}O_{1.9}$	Carbonate Coprecipitation	73.8

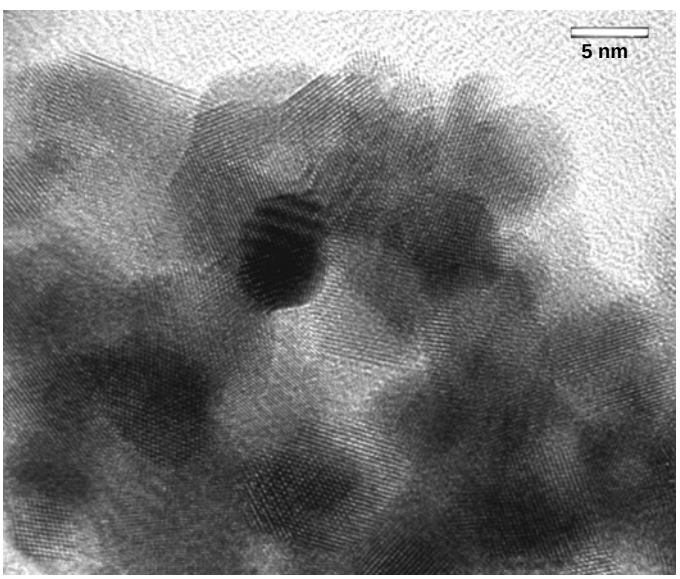

Figure 4. The TEM image of $Au/MgO/Ce_{0.8}Sm_{0.15}Gd_{0.05}O_{1.9}$.

Conclusions

We have developed a new water-gas shift catalyst, $Au/MgO/Ce_{0.8}Sm_{0.15}Gd_{0.05}O_{1.9}$, which is non-pyrophoric and has high WGS activities at low temperature (below 300 ^oC). This nanocystalline(<10nm) $Au/MgO/Ce_{0.8}Sm_{0.15}Gd_{0.05}O_{1.9}$catalyst was synthesized by carbonate co-precipitation of doped ceria followed by gold deposition with urea. The durability of Sm- and Gd-doped ceria as low-temperature water-gas shift (WGS) catalysts was tested with argon gas saturated with water at elevated catalyst temperatures. The SEM and BET surface area analysis indicated that there were no significant changes at 350°C for 10 hours. We have evaluated the WGS activities of various ceria-based catalysts containing Au, Sm, Gd, Zr and Mg. Our results indicate that the presence of Au and MgO in $Au/MgO/Ce_{0.8}Sm_{0.15}Gd_{0.05}O_{1.9}$ plays significant roles in the WGS reaction.

Acknowledgement. This work was supported by FY03 Army Research Laboratory Director's Research Initiative (DRI) Award. Dr. Mattew Ervin and Dr. Wendy Sarney have provided help in electron microscopy.

References

(1) Krummenacher, J. J., West, K. N. and Schmidt, L. D., *J. Catalysis* **2003**, *215*, 332.
(2) Cable, T. L., Brakas, A. B., Ruhl, R. C. and Milliken, C. E., US Patent 6,238,816 (**2001**).
(3) Fu Q, Saltsburg, H. and Flytzani-Stephanopoulos, M., *Science* **2003**, *301*, 935.
(4) Cameron, D., Holliday, R. and Thompson, D., *J. Power Sources* **2003**, *118*, 298.
(5) Sakurai, H., Ueda, A., Kobayashi, T. and Haruta, M., *Chem. Commun.* **1997**, *3* , 271.
(6) Andreeva, D., Idakiev, V., Tabakova, T., Ilieva, L., Falaras, P., Bourlinos, A. and Travlos, A., *Catalysis Today* **2002**, *72*, 51.
(7) Fu, Q., Weber, A. and Flytzani-Stephanopoulos, M., *Catalysis Letters* **2001**, *77*, 87.
(8) Zalc, J. M., Sokolovskii, V. and Loffler, D. G., *J. Catalysis* **2002**, *206*, 169.
(9) Kim, C. H., Bej, S. K. and Thompson, L. T., AIChE 2002 Annual Conference.
(10) Pati, R. K., Lee, I. C., Chu, D. and Ehrman, S. H., *Preprint Paper-American Chemical Society, Division of Fuel Chemistry* **2003**, *48*, 812.
(11) Li, J., Ikegami, T., Mori, T. and Wada, T., *Chem. Mater.* **2001**, *13*, 2913.
(12) Twigg, M. V. and Spencer, M. S., *Applied Catalysis A: General* **2001**, *212*, 161.
(13) Lindstrom, B. AND Pettersson L. J., *Catalysis Letters* **2001**, *74*, 27.
(14) Duprez, D. and Descorme, C. In *Catalysis by Ceria and Related Materials*; Trovarelli, A. , Ed.; Imperial College Press: London, 2002; pp. 243-280.
(15) Trovarelli, A., Boaro, M., Rocchini, E., de Leitenburg, C. and Dolcetti, G., *J. Alloys and Compounds* **2001**, *323*, 584.
(16) Guzman, J. and Gates, B. C., *J. Phys. Chem. B* **2002**, *106*, 7659.